FUNDAMENTAL STUDIES OF NEURAL STIMULATING ELECTRODES

Second Quarterly Report
Covering Period November 29, 1994 to February 28, 1995
CONTRACT NO. N01-NS-4-2310

L. S. Robblee
S. F. Cogan
T. L. Rose
U. M. Twardoch
G. S. Jones
R. B. Jones

EIC Laboratories, Inc.
111 Downey Street
Norwood, Massachusetts 02062

Prepared for
National Institutes of Health
National Institute of Neurological
Disorders and Stroke
Bethesda, Maryland 20892

April, 1995

This QPR is being sent to you before it has been reviewed by the staff of the Neural Prosthesis Program

TABLE OF CONTENTS

LIST OF FIGURES

LIST OF TABLES

1.0 INTRODUCTION AND SUMMARY

This report describes the work on NINDS Contract No. N01-NS-4-2310 during the period November 29, 1994 to February 28, 1995. As part of the Neural Prosthesis Program, the broad objectives of the present fundamental studies are: 1) to evaluate the electrochemical processes that occur at the electrode-electrolyte interface during pulsing regiments characteristic of neural prosthetic applications, 2) to establish charge injection limits of stimulation electrode materials which avoid irreversible electrochemical reactions, 3) to develop an *in vitro* method, which can be applied *in vivo*, for determining the electrochemical real area and stability of microelectrodes; 4) to develop new materials which can operate at high stimulation charge densities for microstimulation, and 5) to provide electrochemical and analytical support for other research activities in the Neural Prosthesis Program at NINDS.

Electrochemical studies of Ir microelectrodes submitted by U. Michigan and Laboratory for Neural Control, NINDS were continued this quarter. A U. Michigan probe which was known to have a slight electrolyte penetration was intentionally selected for stability studies in order to compare the ability of different electrochemical methods to recognize the onset of deterioration in electrode integrity and to identify the underlying causes of changes in electrode properties during long term soaking. The scan rate studies utilizing mass transport of Ru hexaammine provide the most diagnostic information, not only for recognizing that a potential problem exists, but also enables inferences about the source of the problem. For the probe under study this quarter, several weeks soaking in saline electrolyte led to a 5-fold increase in electrochemical dimensions measured under slow scan rate conditions but without a comparable increase under fast scan rate conditions. This disparity between slow and fast scan rate measurements suggests that the slow scan rate response was the sum of responses of individual sites. Measurements of apparent capacitance were consistent with an increase in surface area, as was the impedance and phase angle at frequencies < 20 Hz. The 1 kHz impedance and phase angle gave somewhat contradictory results, the former indicating a decrease in site area with the phase angle suggesting a lower capacitance. These studies are continuing with the goal being the development of a method for monitoring microelectrode integrity *in vivo*.

Dual hat pin electrodes received by Mr. M. Bak, NINDS, Laboratory for Neural Control were studied for nearly 2 months. These electrodes were fabricated using a modified deposition of Parylene and laser ablation of Parylene for tip exposure. One electrode pair which was evaluated in three scan rate studies with Ru hexaammine showed an improved stability of their electrochemical dimensions during the 50 days soaking compared to previously tested hat pin electrodes. A second electrode pair, which had been subjected to a high voltage "burn" to attempt to straighten bent tips, was submitted to determine primarily if the tip straightening procedure altered the electrochemical properties. Unfortunately, the electrodes were damaged and the leads broke during the initial phase of testing. However, initial scan rate studies indicated a larger electrochemical surface area for this electrode pair than for the pair not subjected to the high voltage "burn" suggesting that the tip straightening procedure may also have produced some roughening of the surface. SEMs of this electrode revealed a rough surface texture and also indicated that the Parylene might not have been removed around the entire circumference of the tip. Additional electrodes must be evaluated before conclusions can be drawn about the efficacy of the Parylene removal procedure and the tip straightening protocol.

2.0 Ir MICROELECTRODE STUDIES

Ir microelectrode studies this quarter included evaluation of electrochemical surface areas and stability of sputtered Ir sites on a U. Mich. silicon based probe and of dual hatpin Ir microelectrodes fabricated by M. Bak, NINDS. The electrodes tested are identified as follows:

1. U. Michigan probe CN8-4 with five sputtered Ir sites each having a geom. surface area of 800 μm².
2. Dual hatpin Ir microelectrodes from M. Bak, NINDS. These are identified as BAK-11 and BAK-BRN.

The site identification of the U. Mich. probe is illustrated diagrammatically in Figure 2.1. A dual hatpin microelectrode from M. Bak is illustrated in the low magnification SEM in Figure 2.2. This structure consists of two Ir wire shafts with attached Au lead wires. The junction of the Au wires and the Ir shafts are encased in a bead of epoxy to provide mechanical stability of the junction. The microelectrodes have nearly conical shaped tips with tip exposures of ~23-31 μm in length and radii at the widest part of the cone of ~3-4 μm.

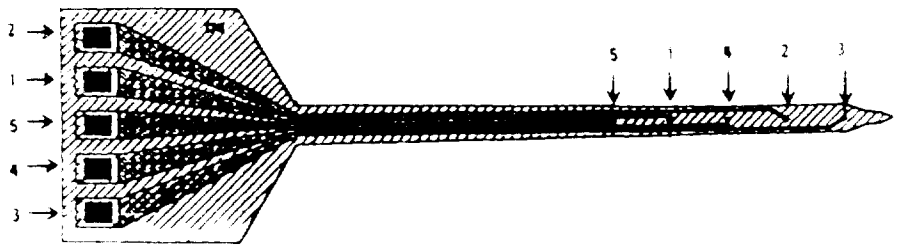

Figure 2.1 Diagrammatic representation of U. Michigan probe identifying location of sites.

Figure 2.2 Low magnification SEM of M. Bak dual hatpin microelectrode. 20X.

U. Michigan Probe CN8-49

The previous quarterly report described in detail the long term stability of activated and unactivated sputtered Ir sites on multi-site probe CN8-48 from U. Michigan. That probe had been selected for long term stability studies of activated and unactivated sites because 4 of the 5 sites of the probe gave a typical faradaic response to Ru hexaammine ($Ru(NH_3)_6Cl_3$) during preliminary stability tests. In the present quarter, U. Michigan probe CN8-49, from a different sputter deposition run, was chosen for study even though only a single site had a normal faradaic response to Ru hexaammine in preliminary stability tests. The overall strategy in this study of probe CN8-49 involved first a scan rate study of one site in Ru hexaammine solution, periodic impedance measurements and cyclic voltammetry of all sites in PBS electrolyte, and a repeat scan rate study of one site. This probe, having sites with varying electrochemical response in initial testing seemed to be a good candidate to evaluate the long term properties of good sites as well as possibly defective sites.

Experimental Methods

A new approach to mounting the U. Mich. probes for long term testing was adopted this quarter. First the probe stalk and contact pad area were coated with dental wax to prevent electrolyte penetration to these areas as described previously (Quarterly Progress Report No. 12, Contract No. N01-NS-1-2300). The probe was held in place in a Bioanalytical Systems Inc. (BAS) Kel-F cell top with wax. The cell top was then placed on the BAS glass cell and held in place with wax. The cell was filled with solution by syringe and the counter electrode and the BAS Ag/AgCl 3M NaCl reference electrode were inserted through other openings in the cell top. Once the cell with electrodes was assembled, it was not dismantled until the end of the test period with the exception of the reference electrode which was removed from solution during periods of passive soaking. This was done to prevent possible contamination of the solution by Ag^+ ions migrating across the reference electrode junction. The cell was placed in the Faraday cage and electrodes connected to the instrumentation. The solution was deaerated for at least 15 minutes prior to cyclic voltammetry measurements by bubbling Ar gas through the solution.

Solutions were changed by using a syringe equipped with flexible tubing to extract solution from the cell, and to replenish the cell with new solution. When changing from Ru solutions to PBS, or *vice versa*, the cell was flushed several times with the incoming solution.

Initial stability testing using cyclic voltammetry at a scan rate of 0.05 V/sec in a solution of 1.28 mM Ru hexaammine in PBS demonstrated that sites 3, 4 and 5 were obviously leaky from the start. This is evidenced by the slightly skewed voltammograms shown in Figure 2.3. Sites 1 and 2 maintained a typical sigmoidal shape of the voltammogram with site 1 giving the most reproducible current over 2 hours of testing.

At the completion of initial stability tests, impedance spectroscopy measurements were taken (the same day) of each site in the Ru hexaammine solution. These measurements were made with site potentials fixed at 0.1 V vs. the reference electrode so that faradaic reactions of the $Ru(NH_3)_6$ were unlikely. The scan rate study was performed on the following day. During the overnight interval, the probe was maintained in the cell containing the Ru hexaammine solution with slow Ar gas bubbling for deaeration. A 2 hour period of stability testing resulted in voltammograms for site 1 that were nearly identical to those obtained in the first stability test on the previous day. Therefore, site 1 was selected as the candidate site for a scan rate study to evaluate electrochemical characteristics.

Results and Discussion

Scan Rate Study No. 1, 24 to 30 hrs in solution

In study 1, the CVs taken at at scan rates up to 0.2 V/s were wave shaped. At scan rates up to 0.005 V/s a plateau current, independent of scan rate, was observed and the forward and reverse curves were coincident. This behavior at low scan rates is consistent with a site behaving like a disk electrode under conditions of spherical diffusion [Fang and Leddy, 1995]. At scan rates above 0.2 V/s, the CVs had distinct cathodic and anodic peaks. The voltammetric data in Table 1 show that the current function, $i_p/v^{1/2}$, decreases as scan rates are increased from 0.001 to 10 V/sec, behavior which is also consistent with non-linear diffusion. However, the current function never attains a limiting value, which would signal the transition to linear diffusion, but instead reaches a minimum at 10 V/sec and then increases with further increases in scan rate. The cathodic peak potential tends to move more cathodic as scan rates increase above 5 V/s. The

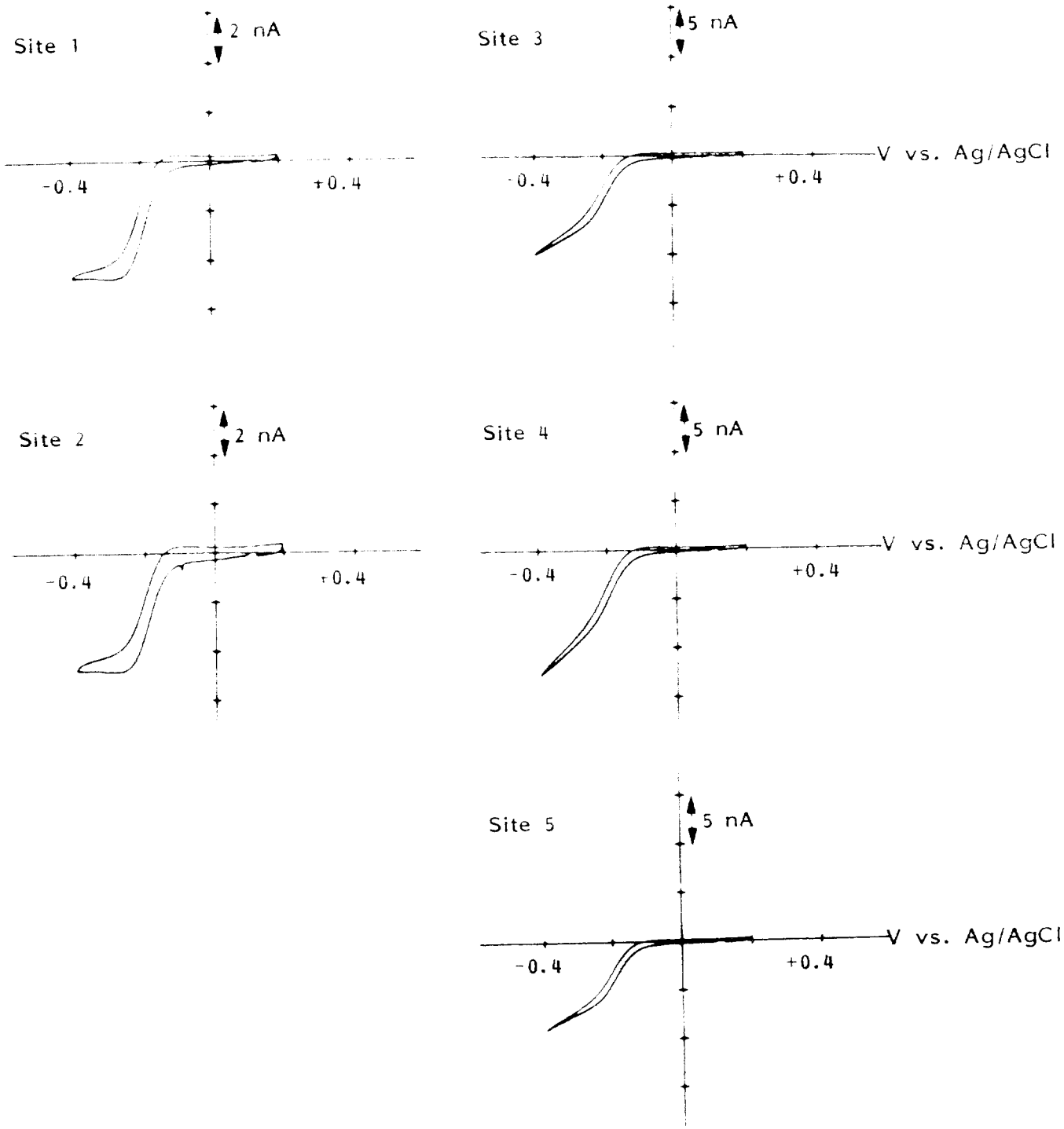

Figure 2.3 Initial cyclic voltammograms acquired at sites 1-5 on U. Michigan probe CN8-49 in the solution of 1.18 mM $[Ru(NH_3)_6]^{3+}$ in PBS. Scan rate = 0.05 V/s.

half-peak potential varies only by 10 mV over the range of scan rates from 0.001-10 V/s, but shifts to a more cathodic value above 20 V/s. These changes in current function and peak potentials suggest the occurrence of some electrolyte penetration into or beneath the sputtered Ir film [Edwards, 1994].

Table 2. Cyclic voltammetric data for the reduction process in the solution of 1.18 mM $Ru(NH_3)_6Cl_3$ in PBS buffer solution at U. Mich. CN8-49, site 1
Scan rate study No. 1

Scan Rate, v (V/s)	Peak Potential E_{pc} (V)	Peak Potential E_{pa} (V)	Half-Peak Potential $E_{p/2}$ (V)	i_p (A)	Current Function χ ($AV^{-1/2}s^{1/2}$)
0.001			-0.190	4.040E-09	1.278E-07
0.002			-0.190	4.000E-09	8.944E-08
0.005			-0.190	4.060E-09	5.742E-08
0.010			-0.190	4.200E-09	4.200E-08
0.020			-0.190	4.300E-09	3.041E-08
0.050			-0.190	4.400E-09	1.968E-08
0.100			-0.180	5.000E-09	1.581E-08
0.500	-0.220	-0.140	-0.190	6.620E-09	9.362E-09
1.000	-0.240	-0.150	-0.180	8.500E-09	8.500E-09
2.000	-0.240	-0.150	-0.180	1.175E-08	8.308E-09
5.000	-0.240	-0.160	-0.180	1.700E-08	7.602E-09
10.000	-0.250	-0.160	-0.190	2.200E-08	6.956E-09
20.000	-0.280	-0.160	-0.200	3.500E-08	7.826E-09
50.000	-0.280	-0.170	-0.200	5.625E-08	7.955E-09
100.000	-0.290	-0.170	-0.200	9.000E-08	9.000E-09
200.000	-0.300	-0.160	-0.200	1.250E-07	8.839E-09

Potential E vs. Ag/AgCl 3M NaCl

Scan Rate Study No. 2, 20 days in solution

During the period between the first and second scan rate studies, the probe was maintained undisturbed in PBS solution (room temperature) except for impedance spectroscopy measurements which were made after 11 days of soaking. In contrast to the results obtained in scan rate study 1, the CVs in study 2 were waveshaped up to 0.1 V/s but the forward and reverse curves did not coincide. A steady state current, independent of scan rate, was observed over the

scan rate range between 0.001-0.005 V/s, but the current was nearly 5 times higher than the plateau current observed in study 1. This difference in current is not accountable for by differences in Ru concentration. Distinct cathodic and anodic peaks were evident only at scan rates of 2 - 50 V/s. The voltammetric data for this study, given in Table 2.2, show a complex dependency of current function on scan rate. The current function decreases with increasing scan rate over the range 0.02 – 2 V/s, is constant for 2 V/s and 5 V/s, and then decreases further between 5 – 50 V/s. At scan rates of 100 and 200 V/s, the residual currents measured in PBS were slightly larger than those measured in the Ru solution. The disparity in residual currents

Table 2.2 Cyclic voltammetric data for the reduction process in the solution of 1.195 mM $Ru(NH_3)_6Cl_3$ in PBS buffer solution at U. Mich. CN8-49, site 1. Scan rate study No. 2

Scan Rate, v (V/s)	Peak Potential E_p (V)	Peak Potential i_p (V)	Half-Peak Potential $E_{p/2}$ (V)	i_p (A)	Current Function $i_p/v^{1/2}$ ($AV^{-1/2}s^{1/2}$)
0.005			-0.210	1.90E-08	6.008E-07
0.002			-0.210	1.95E-08	4.360E-07
0.005			-0.200	1.90E-08	2.687E-07
0.010			-0.200	2.00E-08	2.000E-07
0.020			-0.200	2.05E-08	1.450E-07
0.050			-0.200	2.20E-08	9.839E-08
0.100			-0.190	2.35E-08	7.431E-08
0.200	-0.290	-0.140	-0.190	2.70E-08	6.037E-08
0.500	-0.270	-0.140	-0.190	3.35E-08	4.738E-08
1.000	-0.270	-0.160	-0.190	4.20E-08	4.200E-08
2.000	-0.280	-0.160	-0.190	5.40E-08	3.818E-08
5.000	-0.290	-0.160	-0.200	8.63E-08	3.857E-08
10.000	-0.300	-0.140	-0.210	1.05E-07	3.320E-08
20.000	-0.350	-0.140	-0.210	1.39E-07	3.108E-08
50.000	-0.380	-0.130	-0.210	2.08E-07	2.934E-08
*100.				2.80E-07	2.800E-08
*200.				2.31E-07	1.635E-08

Potential E vs. Ag/AgCl 3M NaCl

*Background currents measured before the wave are larger in blank PBS than those measured in the presence of Ru

at these scan rates leads to an overcorrection of the faradaic current so that voltammetric quantities at these scan rates may be unreliable. The peak potentials at scan rates up to 50 V/s are more cathodic than those observed in study 1, and they shift anodically before reversing to become more cathodic at scan rates above 10 V/s. The half-peak potential also has a complex relationship to scan rate, shifting in the anodic direction up to 2 V/s and then shifting in the cathodic direction at higher scan rates. These voltammetric data are not typical for a disk electrode over the range of scan rates employed. The difference in voltammetric behavior between the two studies indicates a deterioration of the Ir site integrity.

Comparison of electrochemical and geometric dimensions of site 1

The electrochemically determined dimensions obtained in the two scan rate studies are summarized in Table 2-3. For scan rate study 1, the dimensions based on steady state and transient measurements over the scan rate range from 0.1 to 10 V/sec are in good agreement with each other, and they are of approximately the same magnitude as the dimensions of the Ir site as fabricated. However, the surface area calculated from apparent capacitance is higher than that determined from the faradaic measurements, suggesting the presence of some degree of porosity or surface roughness of the sputtered Ir.

The results of scan rate study 2 are in marked contrast to those of study 1. The value of r_{ss} found in study 2 is ~5 times higher than that found in study 1. The radius based on steady state measurements, r_{ss}, is ~6 times higher than that based on transient measurements over the scan rate range from 0.02 to 2 V/s. The "surface area" calculated from r_t is many times larger than the area determined from the linear $iv^{1/2}$ vs. $v^{1/2}$ plot for scan rates 0.02 to 2 V/s. The different values for steady state and transient measurements of radius might result if the electrochemical responses at slow scan rates were due to a contribution from more than one site, and the responses at fast scan rates reflected the contribution of a single site. This type of behavior might be observed in an array of individual microelectrode sites which were connected in parallel. At slow scan rates, overlapping diffusion profiles of individual sites result in a steady state current equal to the sum of the currents at individual sites. At high scan rates, diffusion profiles would be limited to individual sites, and the value obtained for the radius would equal the average value of the radii of individual sites. One way this might occur with the multi-site U. Michigan probe

would be via penetration of electrolyte beneath the sites, or beneath the dental wax and epoxy encapsulation over the contact pads, resulting in electrical continuity between individual sites.

Table 2-5 Dimensions of Ir site No. 1 on the Michigan Probe CN8-49

Study No. Years Elapsed	Dimensions (as fabricated)		Dimensions from Electrochemical Measurements					
			Steady State		Transient Non-linear Diffusion[C]		Transient, Linear Diffusion	from C_{app}[D]
	r - μm	A - μm²	r, μm (disk)	A - μm² (disk)	r - μm	A - μm²	A - μm²	A - μm²
Study 1, 24 hrs	16	800	13	547	10	621		1711
Study 2, 28 days	16	800	62	12080	10	2881	4589	5780

Footnotes to the table:

A Values for r are obtained from the average of the steady state currents observed at 0.001 to 0.005 V sec according to the relationship $r = i_{ss}/nFCD$. The values for A are calculated using the electrochemically determined value of r in the formula for area of a circle.

B A and r are obtained from the slope and intercept of the linear portion of a plot of $iv^{-1/2}$ vs. $v^{1/2}$ over the range of sweep rates from 0.01 - 10 V/s in study 1 and from 0.02 to 2 V/sec in study 2, in accordance with the equation

$$i_T = (2.69 \times 10^5) n^{3/2} A C D^{1/2} v^{1/2} + (0.724 \times 10^5) n \frac{nFCD}{r}$$

C A is obtained from the average of the current functions, $i_T v^{-1/2}$, over the range of sweep rates where they were observed to be constant, i.e. 2-5 V/s according to the equation:

$$i_T = (2.69 \times 10^5) n^{3/2} A C D^{1/2} v^{1/2}$$

D C_{app} is calculated from the residual current at 0 V at the highest scan rate employed, generally 200 V/sec, using the relationship $C_{app} = i/v$. Area is determined from C_{app} assuming a value of 25 μF/cm² for the capacitance of the Ir metal surface.

Impedance Spectroscopy

Impedance spectra were acquired over the range of frequencies from 0.1 Hz to 100 kHz, however for consistency with data presented by other laboratories, only the magnitude and phase angle at 1 kHz are listed in Table 2.4. The initial impedances for the five sites ranged from 325 to 781 kΩ initially with phase angles of 73-78° indicating a large capacitive contribution. During soaking, the impedance of each site decreased gradually so that by day 28, site impedances were nearly the same, ranging from 125 to 165 kΩ. The decrease in site impedance during prolonged soaking is consistent with the increase in electrochemical dimensions found in the scan rate studies using the faradaic reduction of Ru hexaammine. However, the phase angle

data at 1 kHz suggests a decrease in capacitive contribution which appears to contradict the changes indicated by the scan rate studies.

Table 2.4 Impedance (kΩ) and Phase Angle at 1 kHz of Ir sites on Probe CN8-49.

Time	Conditions during Impedance Measurement	Site 1	Site 2	Site 3	Site 4	Site 5
Day 1	Take initial impedances in PBS	494	325	781	399	727
	$Ru(NH_3)_6Cl_3$ @ 100 mV vs Ag/AgCl	-76.51	-73.87	-76.35	-72.66	-77.84
Day 8	Impedances taken in PBS	478	281	471	346	532
	$Ru(NH_3)_6Cl_3$ @ OCP, 40 - 100 mV	-54.34	-62.02	-53.29	-57.95	-47.41
Day 13	Impedances done in PBS @ 100 mV	232	192	295	213	243
		-45.75	-60.22	-51.15	-56.36	-46.52
Day 20	Impedances done in PBS @ 100 mV	155	155	257	204	159
		-64.89	-65.05	-49.86	-55.29	-61.47
Day 28	Impedances done in PBS @ 100 mV	125	133	165	144	130
		-61.78	-62.84	-60.15	-60.60	-62.20

To try to reconcile results obtained by different methods of measurement, we examine the plots of the entire frequency spectrum of impedance and phase angle. In these plots (Figure 2.4), we see that the impedance and phase angle spectra for the five sites become more similar to each other with prolonged soaking. For sites 1 and 2, the initially non-leaky sites, the first impedance plot is linear over the entire frequency spectrum. With increasing soaking time, the linear plots shift downward to lower impedance values but with the same slope as observed initially at frequencies > 20 Hz. After 8 days soaking, a plateau is seen in the impedance curve which extends from ~ 50-100 Hz to ~ 5000 Hz. At frequencies above 5 kHz, the linear plot resumes with the same slope as at lower frequencies. After 20 days soaking, this plateau is shifted toward higher frequencies. In contrast, the initial impedance plots for sites 3, 4 and 5 are not linear over the entire frequencey spectrum, but have a plateau extending between 5 to 50 Hz. These initial plots are similar to each other but different from those of sites 1 and 2. After soaking for a period of time, the impedance plots of sites 3, 4 and 5 become similar to those of sites 1 and 2.

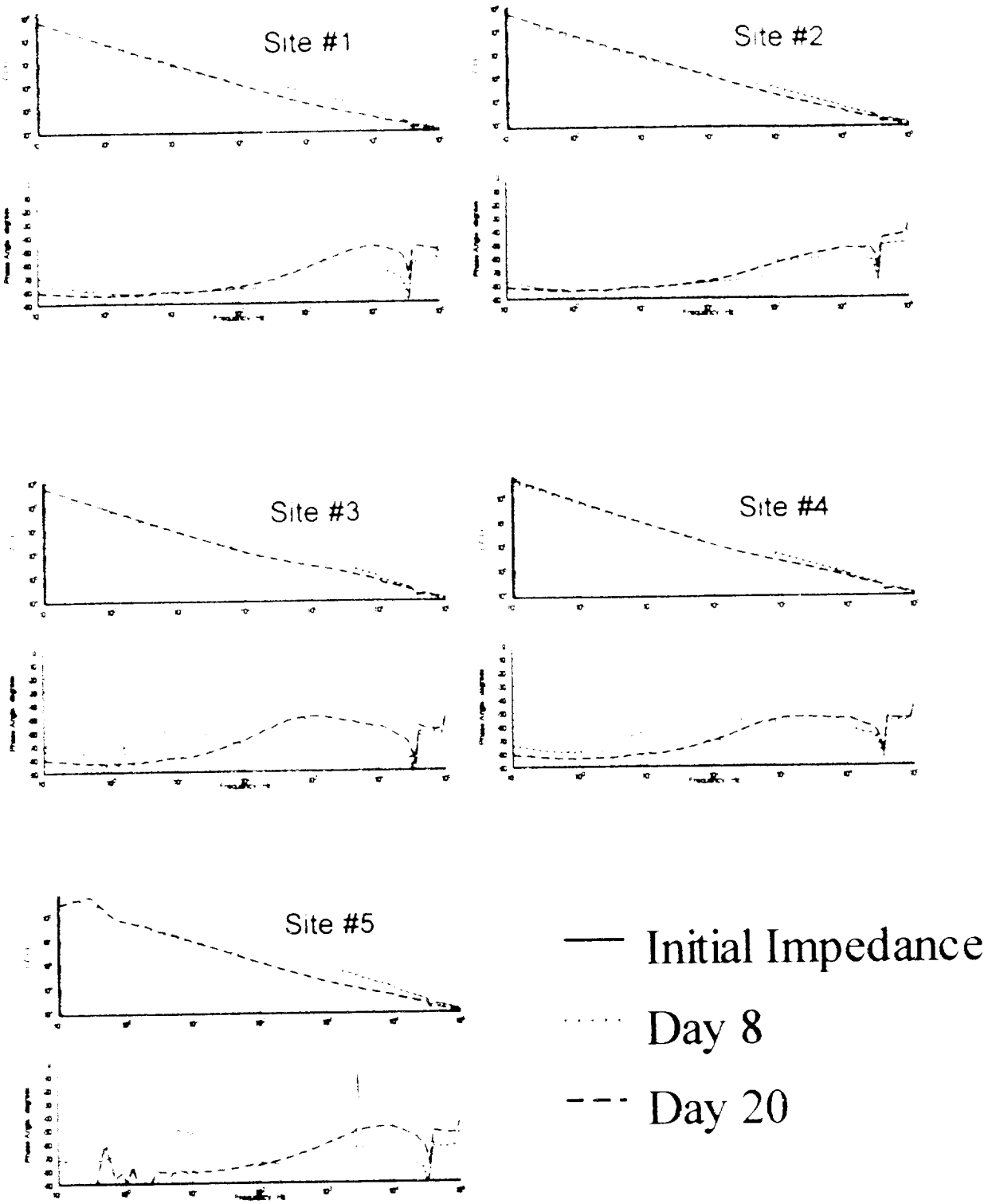

Figure 2.4 Impedance and phase angle of sites on U. Michigan Probe CN8-49 at different times of storage

The initial frequency spectra of phase angle also fall into two categories: those for sites 1 and 2 are similar to each other, and those of sites 3, 4 and 5 are similar. After varying periods of soaking, these all become more alike with phase angles changing from capacitive to more resistive values over the frequency range from 20 Hz to 5 kHz. At low frequencies, all sites show a shift in phase angle toward -90° which is consistent with an increase in capacitive behavior. These results suggest that impedance and phase angle measurements at low frequency, e.g. 100 Hz, correlate better with the changes in electrode dimensions observed in slow scan rate Ru hexaammine studies, and thus may be more appropriate for detecting changes in electrode properties caused by electrolyte penetration than measurements at 1 kHz.

Dual Hatpin Ir Microelectrodes

Two sets of dual hatpin Ir microelectrodes were submitted by Mr. M. Bak, NINDS, for electrochemical characterization. These electrodes were insulated with Parylene which was deposited with an adhesion primer and removed using an excimer laser. After the Parylene removal, the tips were "bubble" tested to remove residual primer which is not readily taken off by the laser. Electrode impedances were measured at 1 kHz before and after this "bubble" test. The electrode tips on one array, identified as "BRN" had become bent during fabrication and were subjected to a high voltage "burn" to try to straighten them. One of the questions we were asked to answer was whether this "burn" had a deleterious effect on the electrodes.

Each dual hatpin microelectrode array, as submitted, was held in a glass capillary tube with the epoxy butt and electrode shafts extending from one end, and the Au lead wires extending from the other. In order to stabilize these devices, we encased each end of the glass tube in dental wax thereby preventing the array from sliding out of the tube, and preventing electrolyte solution from filling the tube. The array was mounted in a semi-permanent manner in a BAS electrochemical cell using wax similar to the way in which the U. Mich. probe was mounted. Solutions were introduced into the cell and removed by syringe. Once the array was assembled in the cell and exposed to electrolyte solution, it was not removed until test protocols were completed. At this time, electrode #11 remains in solution. Electrode BRN has been removed and testing terminated due to breakage of the Au lead wires.

Electrochemical characterization included scan rate studies of the faradaic reduction of Ru hexaammine and impedance spectroscopy at various intervals during long term soaking. Tables 2.9 to 2.10 summarize the voltammetric data for BAK microelectrodes 11A and 11B. These data were obtained in three scan rate studies which were performed at different times over a span of 50 days. Tables 2.11 and 2.12 summarize the voltammetric data for BRN-A and BRN-B.

Steady state currents were observed at BAK-11 electrodes at scan rates up to 0.01 or 0.02 V/s in the three scan rate studies. The voltammograms in this scan rate range were wave shaped with the currents on the forward and reverse scans coinciding in most studies. This is a more rapid approach to steady state behavior than was observed with the UM Michigan electrode and may be due to the geometry of the electrode and the small thickness of insulator relative to electrode diameter [Fang and Leddy, 1995]. At scan rates above 0.01 or 0.02 V/s, residual currents in PBS were higher than those in Ru solution resulting in an overcorrection of the faradaic current by background subtraction. Thus, the voltammetric data at high scan rates are not suitable for numerical analysis. They are given here primarily to compare the trends in current function and peak potential behavior over time.

Table 2.5 Cyclic voltammetric data for the reduction process in the solution of 1.58 mM $Ru(NH_3)_6Cl_3$ in PBS buffer solution at M. Bak electrode I.I.A. scan rate study 1.

Scan Rate (V/s)	Peak Potential E_{pa} (V)	Peak Potential E_{pc} (V)	Half-Peak Potential $E_{1/2}$ (V)	i_{pc} (A)	Current Function $i_{pc}/Av^{1/2}$ ($AV^{-1/2}s^{1/2}$)
0.001			-0.210	5.2E-09	1.644E-07
0.002			-0.210	5.2E-09	1.163E-07
0.005			-0.210	5.2E-09	7.354E-08
0.01			-0.210	5.3E-09	5.300E-08
0.02			-0.210	5.3E-09	3.748E-08
0.05			-0.210	5.2E-09	2.325E-08
0.10			-0.210	5E-09	1.581E-08
0.20			-0.200	5.3E-09	1.185E-08
0.50	-0.290	-0.130	-0.200	5.7E-09	8.061E-09
1.00	-0.300	-0.130	-0.200	6.2E-09	6.200E-09
2.00	-0.290	-0.140	-0.200	7E-09	4.950E-09
5.00	-0.280	-0.140	-0.200	8.8E-09	3.935E-09

*Background currents measured before the wave are larger in blank PBS than those measured in the presence of Ru for scan rates 0.01-100 V/s

Table 2.6 Cyclic voltammetric data for the reduction process in the solution of 1.74 mM $Ru(NH_3)_6Cl_3$ in PBS buffer solution at M. Bak electrode I.I.A. scan rate study 2.

Scan Rate (V/s)	Peak Potential E_{pa} (V)	Peak Potential E_{pc} (V)	Half-Peak Potential $E_{1/2}$ (V)	i_{pc} (A)	Current Function $i_{pc}/Av^{1/2}$ ($AV^{-1/2}s^{1/2}$)
0.001			-0.210	4.40E-09	1.391E-07
0.002			-0.200	4.40E-09	9.839E-08
0.005			-0.210	4.40E-09	6.223E-08
0.01			-0.200	4.70E-09	4.700E-08
0.02			-0.200	4.50E-09	3.182E-08
0.05			-0.210	4.60E-09	2.057E-08
0.10			-0.200	5.00E-09	1.581E-08
0.20			-0.200	6.00E-09	1.342E-08
0.50		-0.120	-0.200	6.40E-09	9.051E-09
1.00		-0.140	-0.200	7.50E-09	7.500E-09
2.00			-0.200	9.25E-09	6.541E-09
5.00			-0.190	1.40E-08	6.261E-09

*Background currents measured before the wave are larger in blank PBS than those measured in the presence of Ru for scan rates greater than 0.01 V/s

Table 2.7 Cyclic voltammetric data for the reduction process in the solution of 1.24 mM $Ru(NH_3)_6Cl_3$ in PBS buffer solution at M. Bak electrode 11A, scan rate study 3.

Scan Rate (V/s)	Peak Potential E_{pc} (V)	Peak Potential E_{pa} (V)	Half-Peak Potential $E_{1/2}$ (V)	i_p (A)	Current Function $i_p/v^{1/2}$ ($AV^{-1/2}s^{1/2}$)
0.001			-0.210	3.70E-09	1.170E-07
0.002			-0.210	4.00E-09	8.944E-08
0.005			-0.210	4.00E-09	5.657E-08
0.010			-0.210	4.20E-09	4.200E-08
0.020			-0.210	4.50E-09	3.182E-08
0.050			-0.210	4.60E-09	2.057E-08
0.100			-0.200	4.20E-09	1.328E-08
0.200			-0.190	5.40E-09	1.207E-08
0.500			-0.190	5.60E-09	7.920E-09
1.000			-0.190	6.00E-09	6.000E-09
2.000			-0.190	7.25E-09	5.126E-09
5.000			-0.190	1.05E-08	4.696E-09

*Background currents measured before the wave are larger in blank PBS than those measured in the presence of Ru for scan rates 0.01-0.05 V/s and 0.2-5 V/s. No peaks were observed over the entire scan rate range studied

Table 2.8 Cyclic voltammetric data for the reduction process in the solution of 1.58 mM $Ru(NH_3)_6Cl_3$ in PBS buffer solution at M. Bak electrode 11B, scan rate study 1.

Scan Rate (V/s)	Peak Potential E_{pc} (V)	Peak Potential E_{pa} (V)	Half-Peak Potential $E_{1/2}$ (V)	i_p (A)	Current Function $i_p/v^{1/2}$ ($AV^{-1/2}s^{1/2}$)
0.001			-0.210	5.50E-09	1.739E-07
0.002			-0.210	5.40E-09	1.207E-07
0.005			-0.210	5.50E-09	7.778E-08
0.010			-0.210	5.30E-09	5.300E-08
0.020			-0.210	5.40E-09	3.818E-08
0.050			-0.210	5.60E-09	2.504E-08
0.100			-0.200	5.90E-09	1.866E-08
0.200			-0.200	6.00E-09	1.342E-08
0.500			-0.200	6.40E-09	9.051E-09
1.000	-0.290	-0.140	-0.200	6.60E-09	6.600E-09
2.000	-0.280	-0.110	-0.200	7.00E-09	4.950E-09
5.000	-0.290	-0.140	-0.210	9.50E-09	4.248E-09

*Background currents measured before the wave are larger in blank PBS than those measured in the presence of Ru for scan rates 0.01-0.05 V/s and 0.2-200 V/s

Table 2.9 Cyclic voltammetric data for the reduction process in the solution of 1.42 mM $Ru(NH_3)_6Cl_3$ in PBS buffer solution at M. Bak electrode 11B, scan rate study 2.

Scan Rate (V/s)	Peak Potential E_{pc} (V)	Peak Potential E_{pa} (V)	Half-Peak Potential $E_{1/2}$ (V)	i_p (A)	Current Function $i_p/v^{1/2}$ ($AV^{-1/2}s^{1/2}$)
0.005			-0.210	3.80E-09	1.202E-07
0.002			-0.210	3.80E-09	8.497E-08
0.005			-0.210	3.60E-09	5.091E-08
0.01			-0.220	3.70E-09	3.700E-08
0.02			-0.210	4.20E-09	2.970E-08
0.05			-0.220	4.20E-09	1.878E-08
0.1			-0.220	4.20E-09	1.328E-08
0.2			-0.210	4.40E-09	9.839E-09
0.5			-0.210	5.20E-09	7.354E-09
1		-0.120	-0.200	6.00E-09	6.000E-09
2		-0.100	-0.200	8.00E-09	5.657E-09
5			-0.170	1.33E-08	5.948E-09

*Background currents measured before the wave are larger in blank PBS than those measured in the presence of Ru for scan rates greater than 0.01 V/s. No cathodic peaks were observed over the scan rate range studied

Table 2.10 Cyclic voltammetric data for the reduction process in the solution of 1.24 mM $Ru(NH_3)_6Cl_3$ in PBS buffer solution at M. Bak electrode 11B, scan rate study 3.

Scan Rate (V/s)	Peak Potential E_{pc} (V)	Peak Potential E_{pa} (V)	Half-Peak Potential $E_{1/2}$ (V)	i_p (A)	Current Function $i_p/v^{1/2}$ ($AV^{-1/2}s^{1/2}$)
0.005			-0.210	3.10E-09	9.803E-08
0.002			-0.200	3.20E-09	7.155E-08
0.005			-0.200	3.10E-09	4.384E-08
0.01			-0.200	3.30E-09	3.300E-08
0.02			-0.210	3.20E-09	2.263E-08
0.05			-0.200	3.30E-09	1.476E-08
0.1			-0.200	3.60E-09	1.138E-08
0.2			-0.200	3.60E-09	8.050E-09
0.5	-0.510	-0.110	-0.190	4.20E-09	5.940E-09
1	-0.300	-0.140	-0.190	5.17E-09	5.170E-09
2	-0.300	-0.140	-0.180	6.50E-09	4.596E-09
5			-0.150	1.00E-08	4.472E-09

*Background currents measured before the wave are larger in blank PBS than those measured in the presence of Ru for scan rates 0.05-0.2 V/s and 5-200 V/s

Table 2.11 Cyclic voltammetric data for the reduction process in the solution of 1.42 mM $Ru(NH_3)_6Cl_3$ in PBS buffer solution at BAK-BRN-A

Scan Rate, v (V/s)	Peak Potential 1 E_{p1} (V)	Peak Potential 1 E_{p1} (V)	Half-Peak Potential $E_{p/2}$ (V)	i_p (A)	Current Function $i_p/v^{1/2}$ ($AV^{-1/2}s^{1/2}$)
0.100			-0.200	1.150E-08	3.637E-07
0.0625			-0.200	1.075E-08	2.404E-07
0.0625			-0.200	1.200E-08	1.697E-07
0.0313			-0.200	1.100E-08	1.100E-07
0.0200			-0.200	1.075E-08	7.601E-08
0.0150			-0.200	1.275E-08	5.702E-08
0.0100			-0.190	1.250E-08	3.953E-08
0.0050			-0.200	1.250E-08	2.795E-08
0.0025	-0.285	-0.140	-0.190	1.650E-08	2.333E-08

*Background currents measured before the wave are larger in blank PBS than those measured in the presence of Ru for scan rates greater than 1 V/s

Table 2.12 Cyclic voltammetric data for the reduction process in the solution of 1.42 mM $Ru(NH_3)_6Cl_3$ in PBS buffer solution at Ir microelectrode BAK-BRN-B

Scan Rate, v (V/s)	Peak Potential 1 E_{p1} (V)	Peak Potential 1 E_{p1} (V)	Half-Peak Potential $E_{p/2}$ (V)	i_p (A)	Current Function $i_p/v^{1/2}$ ($AV^{-1/2}s^{1/2}$)
0.100			-0.200	5.700E-09	1.802E-07
0.0625			-0.200	5.700E-09	1.275E-07
0.0625			-0.200	5.640E-09	7.976E-08
0.0313			-0.200	5.800E-09	5.800E-08
0.0200			-0.200	6.000E-09	4.243E-08
0.0150			-0.200	6.200E-09	2.773E-08
0.0100			-0.200	6.800E-09	2.150E-08
0.0050			-0.190	7.500E-09	1.677E-08
0.0025	-0.280	-0.120	-0.180	8.500E-09	1.202E-08
0.0016	-0.270	-0.130	-0.140	1.120E-08	1.120E-08
2.000	-0.240	-0.140	-0.150	1.525E-08	1.078E-08
3.000	-0.250	-0.150	-0.170	3.100E-08	1.386E-08

* Data obtained from cyclic voltammograms without correcting for charging and residual current in blank PBS. Electrode lead broke before measurements could be taken in PBS.

The steady state currents observed in the slow scan rate voltammograms were used to calculate the height, h, of the cone using the microscopically measured values for r in the equation for the steady state current at a cone-shaped electrode, $i_{ss} = 4nF(C^*)D\sqrt{(h^2 + r^2)}$. As seen in Table 2.13, the electrochemically determined values for h of electrodes 11A and 11B are much smaller than those measured microscopically. In contrast, the electrochemical measurements of h for BAK-BRN-A and B are a close approximation of microscopic measurements.

Table 2.13 Dimensions of dual hatpin Ir microelectrodes.

Sample ID	Geometric Dimensions (from microscopy)			Electrochemically Determined Dimensions		
	r, μm	h, μm		From Steady State Current		From C_{dl}
		light	SEM	h*, μm (cone)	ESA*, μm (cone)	ESA, μm
BAK-11A, day 2	3.5	28		9.7	114	400, 552
BAK-11A, day 28				9.1	108	856, 896
BAK-11A, day 49						848, 850
BAK-11B, day 8	3.5	27		12.9	147	304, 800
BAK-11B, day 22				9.7	114	1396, 2496
BAK-11B, day 50				9.1	104	760, 1320
BAK-BRN-A, day 1	3.5	23	21	25.2	301	2080, 8000
BAK-BRN-B*, day 1	3.5	27	18	15.1	171	4,800

The radius (r) of 3.5 μm is taken from averages of measurements made from SEMs of BAK-BRN-A and BAK-BRN-B and is assumed to be the same for electrodes 11A and 11B. The optical dimensions for cone height (h) are those provided by M. Bak.

h* of cone is calculated using r in the equation for the steady state current to a cone

$$i_{ss} = 4nF(C^*)D\sqrt{(h^2 + r^2)}$$

ESA* of the cone is calculated from the equation for area of a cone

$$A = \pi r\sqrt{(h^2 + r^2)}$$

A_{geo} is calculated from the residual current, i_c, at 0 V at 200 V/sec, using the relationship $C_{dl} = i_c/v$. Area is determined from C_{dl} assuming a value of 25 mF/cm² for the capacitance of the Ir metal surface. If two values are shown, the lower value represents the capacitance calculated from i_c in the Ru hexaammine solution; the higher value from i_c in blank PBS.

For electrochemical measurements, the tip designations of A or B were assigned by labeling the lead wire used for electrical connections, and these designations may not be the same as those provided with the electrodes. It also was not possible to distinguish between tips A and B in the SEM, again due to lack of facets on the tips themselves. Thus, measurements of cone length made by the three techniques cannot be assigned unambiguously to a specific tip.

It is noteworthy that there is relatively little change in the value of h for BAK-11A and 11B electrodes over relatively long periods of soaking, although there was a slight deterioration in the quality of the voltammograms obtained in study 5. The amount of distortion which is typically associated with a leak at the metal-Parylene junction was not as severe as has been observed in the past. The stability of the dimensions based on steady state currents indicates a greater stability of the electrode geometry than has been observed previously with Parylene insulated metal electrodes and is favorable for further development of the modified fabrication procedures.

An unusual characteristic of the electrochemical response of electrodes 11A and 11B was the consistently higher residual current in PBS compared to that in Ru hexaammine solution at scan rates above 0.01-0.02 V/s. One explanation for the higher residual currents in the absence of Ru hexaammine is that there may be a component of the electrode surface available for capacitive charging in the blank PBS that is blocked by Ru hexaammine. For instance, if there were a thin dielectric layer covering part of the metal, then that portion of the surface might contribute to the charging current in blank PBS, but be blocked by the large Ru hexaammine molecules. Alternatively, the "extra" charging current in blank PBS might arise from surface oxide reactions which also might be hindered by Ru hexaammine. Although electrodes 11A and 11B have not been examined by SEM at this time, the SEMs of the BAK-BRN electrodes demonstrated the patches of a thin coating over the metal surface which appeared to be residual polymer (see Figure 2.5).

Table 2.13 also lists the electrochemical surface areas calculated from the apparent capacitance (C_{ap}) measured at the highest scan rates. These values for surface area are much larger than those obtained from the steady state measurements of faradaic current. The higher values of ESA obtained from C_{ap} may be due to surface roughness of the Ir or the presence of a surface oxide. The "bubble" test that is performed to remove residual primer might promote roughening of the Ir surface or the development of a thin oxide layer. The observed increase in ESA based on C_{ap} suggests that additional surface is being exposed somewhere, either by increasing roughness or oxide formation. Further electrochemical testing of these electrodes is planned as well as SEM studies at the termination of the soaking period which may aid in answering some of the questions raised by the electrochemical measurements.

The electrodes in the BRN array are a special case since they were subjected to a very different treatment prior to being received at UC. It was only possible to perform one scan rate study with each of these due to their leads breaking during testing. As indicated above, the values obtained for Ir are close to those obtained by microscopic measurements. However, the ESA of both BRN electrodes, determined from C_{dl}, is many times higher than that based on steady state measurements of faradaic current, and is much higher than the ESA from C_{app} of electrode 1-A or 1-B. SEM examination of the BRN tips showed severe bending of the Ir shafts (Figure 2.2) which indicates that the electrodes were badly damaged at some time before or during testing. Since it is possible for the integrity of the Parylene coating along the shaft or at the metal-Parylene junction to be compromised if the wires are bent to the extreme seen by SEM, we hesitate to attach to much significance to the large difference in ESAs determined by the different measurements of the BRN electrodes. It will be necessary to test another set of similar electrodes before arriving at definite conclusions regarding the effect of the high voltage "burn" on the electrochemical characteristics of such electrodes.

High magnification SEMs of the BRN electrodes shown in Figure 2.5 show that the Parylene coating was not completely removed from the entire circumference of the conical tip. This "defect" probably can be corrected by modifying the laser ablation process. An additional defect in the tips which is intrinsic to the Ir wire is an apparently deep groove which is oriented lengthwise along the tip. This defect in the wire is now known to have developed at an early stage in the manufacture of the wire and was preserved during the successive wire drawing stages required in fabricating ultra-thin wire. What effect this "groove" might have in terms of charge injection properties and electrochemical stability can only be surmised at this time. The preference is to obtain Ir wire without the defect so that electrochemical issues might be more straightforward.

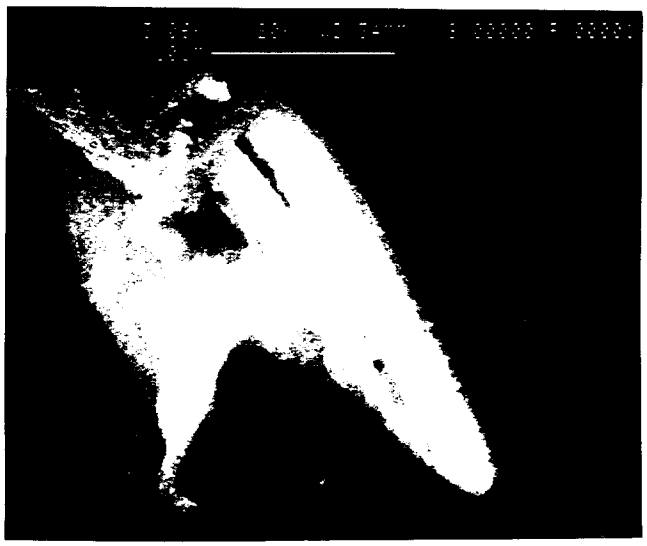

A

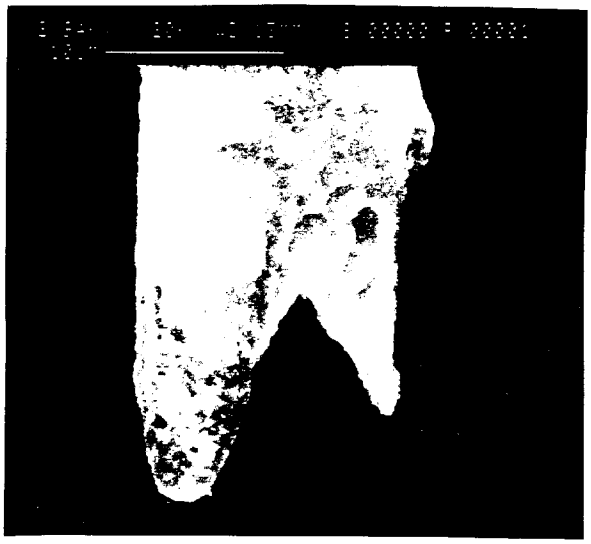

B

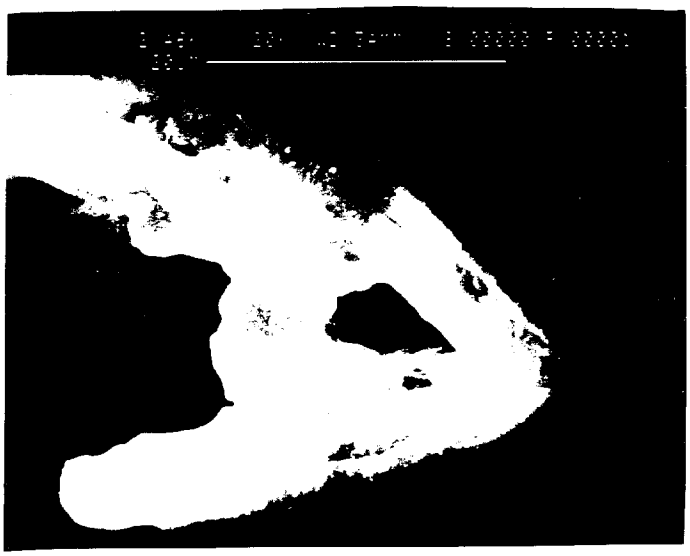

C

D

Figure 2.5 High magnification scanning electronmicrographs of Ir tips on BAK-BRN. Note that it is not possible to distinguish between the A and B tips as specified by Mr. Bak.
Figs. A and B represent opposite sides of the same tip. Note the longitudinal groove in Fig. A and the residual Parylene adhering to one side of the tip.
Figs. C and D represent the other hatpin tip. Note the wide longitudinal groove which seems to be filled with some material. Note also the fragment of what appears to be Parylene still adhering partially to the distal end of the tip.

Impedance Spectroscopy

Impedance spectra were taken of the electrodes 11A and 11B at various intervals during the long term soaking. Table 2.14 summarizes the impedance magnitude at 1 kHz. In contrast to a steady downward trend in impedance such as was observed for the U. Michigan site, the impedance of electrode 11A remained somewhat constant up to day 14, after which it began to increase to values almost equal to Mr. Bak's pre-bubble test level. The impedance of 11B was more erratic, increasing initially to 1.2 MΩ, decreasing to a low of 400 kΩ after 20 days soaking, and increasing again to MΩ levels at 51 days. These electrodes are still soaking and measurements are being taken periodically.

Table 2.14 Impedances (kΩ) at 1 kHz of Ir sites on M. Bak electrode No. 11

Time	Conditions during Impedance Measurement	Site A	Site B
Before 8/16	Measurement by Mr. Bak of initial / before bubble test	1550*	1400*
Before 8/16	Measurement by Mr. Bak of / after bubble test	850*	800*
Day 5	Initial Impedance in PBS @ 100 mV vs Ag/AgCl	893	1287
Day 6	Impedance in PBS @ OCP -140 mV		585
Day 6	Impedance in PBS @ 100 mV		368
Day 7	Impedance in PBS @ OCP -125 mV		374
Day 8	Impedance in PBS @ OCP -125 mV		635
Day 11	Impedance in PBS @ OCP -130 mV		578
Day 12	Impedance in PBS @ OCP: A -79 mV, B -124 mV	831	588
Day 13	Impedance in PBS @ OCP -127 mV	845	
Day 14	Impedance in PBS @ OCP -104 mV	574	
Day 15	Impedance in PBS @ OCP -49 mV	570	
Day 18	Impedance in PBS @ OCP -33 mV	611	
Day 19	Impedance in PBS @ OCP -23 mV	712	
Day 20	Impedance in PBS @ OCP: A -21 mV, B -58 mV	1272	403
Day 5	Impedance in Ru(NH$_3$)$_6$Cl$_3$ PBS @ 100 mV	991	1399
Day 50	Impedance in PBS @ 100 mV	1336	885

* The designation of electrode tips as A or B in Mr. Bak's impedance measurements may not be the same as IIT's identification for reasons given in the notes to Table 2.13.

Conclusions regarding merits of different methods of electrode characterization.

The Ru hexaammine data provides more detailed diagnostic information regarding the characteristics of the individual microelectrodes than a measurement of impedance at the 1 kHz

frequency typically employed by electrode manufacturers. For example, there are indications that the prolonged soaking of probe CNS-49 resulted in the establishment of electrical continuity between the individual sites resulting in their combined contribution to the faradaic current in the slow scan rate studies. This type of information is not immediately obvious from the impedance and phase angle at 1 kHz. However, we recognize that a scan rate study with Ru hexaammine has a very limited application. For example, it cannot be performed with electrodes that are implanted *in vivo*. Therefore, in view of the overall goal of developing electrode characterization methodology suitable for *in vivo* use, we are attempting to establish diagnostic methods for characterizing electrode dimensional stability using other methodology such as impedance spectroscopy. The results presented here demonstrate the value of examining the entire frequency spectrum of impedance and phase angle rather than relying on a single frequency measurement in order to monitor dimensional stability of microelectrodes. We anticipate that further analysis of electrode stability using both of these methods of analysis will provide a baseline of information which can be employed to establish a test protocol for *in vivo* use.

3.0 WORK FOR NEXT QUARTER

The long term soaking studies of CNS8-49 and BAK-11 electrodes are continuing. During the coming quarter, stimulation pulse experiments will be incorporated into the stability studies to evaluate what effect these might have on electrode dimensional stability and impedance. At the termination of the stability studies, both types of electrodes will be examined by SEM to attempt to correlate structural appearance with electrochemical findings.

The impedance spectra of BAK-11 electrodes have not been analyzed fully as yet. For this report, only the 1 kHz impedance values were extracted, but in coming months, other portions of the frequency spectrum will be examined to search for correlations with the Ru hexaammine data.

We anticipate receiving new multi-site probes from U. Michigan with integrated ribbon cables for electrochemical testing. With these probes, we should be able to evaluate the stability of individual sites, *per se*, without any contribution from neighboring sites via electrolyte penetration to the contact pads.

4.0 REFERENCES

Bard, Allen J. and Johna Leddy. 1995. Cyclic voltammetric responses for inlaid microdisks with shields of thickness comparable to the electrode radius. A simulation of reversible electrode kinetics. Anal. Chem. **67**:1259-1270.

Kovacs, Gregory T.A. 1994. Integrity of ultramicro-stimulation electrodes determined from electrochemical measurements. J. Applied Electrochem. **24**:835-857.